Crystallisation of Foturan® glass–ceramics

Anna Evans *, Jennifer L.M. Rupp, Ludwig J. Gauckler

ETH Zurich, Department of Materials, Nonmetallic Inorganic Materials, Wolfgang-Pauli-Strasse 10, CH-8093 Zurich, Switzerland

Abstract

Photostructurable glass–ceramics are suitable for 3-dimensional microfabrication and, in some instances, can be used as an alternative material to silicon in the microfabrication of micro-electro-mechanical-system (MEMS) devices. Foturan® is a photosensitive lithium–aluminium–silicate glass that can be structured by an exposure to UV light, followed by a thermal treatment and an etching step. In this work, the crystallisation kinetics and microstructure evolution of unexposed and UV-exposed Foturan® are investigated by means of differential scanning calorimetry, X-ray diffraction and scanning electron microscopy. The glass transition temperature T_g, the apparent activation energy of crystallisation E_a and the colour of UV-exposed Foturan® are discussed. It is shown that nucleation and crystallisation of UV-exposed Foturan® can be steered either as a function of temperature (non-isothermal) or as a function of time (isothermal). This is essential for the photostructuring and etching of Foturan® regarding the achievable feature sizes of 25 μm for MEMS applications.
© 2011 Elsevier Ltd. All rights reserved.

Keywords: Foturan®; Photostructurable glass ceramic; Nucleation; Crystallisation; MEMS microfabrication

1. Introduction

The miniaturisation of electronic devices requires suitable substrates for micro-electro-mechanical-system (MEMS) fabrication. Currently, mostly silicon is used as in the semi-conductor industry. There are, however, several limitations regarding the processing and applications of silicon, e.g. it is a stiff, brittle and semi-conducting material, and a photoresist and a lithography step are required for the surface structuring. Furthermore, silicon has a thermal expansion coefficient of $2.6 \times 10^{-6} \, \text{K}^{-1}$ (at 20 °C) and is mainly used in low-temperature applications in order to prevent silicon diffusion.

Photosensitive glass is an alternative material used in microfabrication. Such glasses allow for a direct etching and structuring through photo-radiation and thermal annealing steps.[1–3] One example of a commercially available photostructurable glass is Foturan®. The properties and the processing of Foturan® glass offer several advantages compared to the silicon technology: Foturan® is a good electrical insulator, it is thermally stable, and has a thermal expansion coefficient of $8.6 \times 10^{-6} \, \text{K}^{-1}$ (at 20 °C) close to the one of most ceramic oxide thin films and it is possible to achieve high aspect-ratio microstructures.

Foturan® is used in different micro-system components such as micro-reactors and micro-fluidic devices,[4–6] micromechanics,[7–9] gas channels systems made of bonded wafers[10] and substrates for micro-solid oxide fuel cells.[11–15]

An overview of the chemical, thermal, mechanical, and electrical properties of Foturan® is given by Dietrich et al.[10] The state-of-the-art photostructuring of Foturan® glass is always based on: (i) a UV-radiation step by mask photolithography[10] or laser-induced exposure to predefine the selective areas where nuclei are formed in the glass,[16] (ii) followed by a thermal annealing step in which the nuclei a crystallised, and (iii) finally a selective etching step by a wet-chemical agent[10] or by focussed ion beam[17] whereby the crystalline parts are etched faster than the glassy areas to obtain channels through the Foturan® wafers.

Foturan® (Mikroglas Chemtech GmbH, Mainz, Germany) is a photosensitive lithium–aluminium–silicate glass consisting primarily of silica (SiO_2, 75–85 wt.%) and stabilizing oxides, such as Li_2O (7–11 wt.%), K_2O (3–6 wt.%), Al_2O_3 (3–6 wt.%), Na_2O (1–2 wt.%), ZnO (<2 wt.%) and Sb_2O_3 (0.2–0.4 wt.%).[10] It can be microstructured by ultraviolet (UV) lithography fol-

* Corresponding author.
  E-mail address: anna.evans@mat.ethz.ch (A. Evans).

lowed by a thermal treatment and chemical wet etching with hydrofluoric acid.[10] The photosensitivity is achieved by the presence of dopants such as Sb_2O_3, Ag_2O and CeO_2 within the glass matrix. During the exposure to UV light, Ce^{3+} absorbs a photon and is converted to Ce^{4+} and releases an electron. In the subsequent thermal treatment at $500\,^{\circ}C$ and $600\,^{\circ}C$, the Ag^+ ions absorb the electrons and agglomerate to Ag nuclei. The glass crystallises around these Ag nuclei forming a lithium-metasilicate, and proceeds actively to grain formation and growth. It is important to note that crystalline Foturan® grains show a 20 times higher etch rate of around $10\,\mu m/min$ in 10% hydrofluoric acid compared to the amorphous glass.[10] The microstructuring of Foturan® wafers is based on the selective etching rates of the UV-exposed and thermally treated crystalline areas and of the unexposed glassy ones.

The Foturan® crystal size defines the actual feature size of the to-be-structured patterns and the final microfabrication resolution, e.g. the achievable aspect ratio of the geometric structures and the roughness of the etched side walls. This crystal size depends on the UV-exposure time and wavelength, and also on the thermal annealing time and temperature. The annealing program of Foturan® suggested by the Mikroglas company is performed in a two-step tempering consisting of a slow heating ($1\,^{\circ}C/min$) up to $500\,^{\circ}C$ with an 1 h isothermal hold to provoke nucleation and a further 1 h dwell at $600\,^{\circ}C$ to induce crystallisation and grain growth.[10,18] It is reported that this two-step annealing results in actual mean crystal sizes of $1–10\,\mu m$ suitable for microstructuring Foturan® with feature sizes down to $25\,\mu m$.[10] It is important to note that the actual grain growth temperature signifies the maximum temperature the material may be exposed to in further thermal treatments and in MEMS applications. For applications at higher temperatures, Mikroglas suggests an additional annealing of Foturan® at $800\,^{\circ}C$, but the authors do not specify the exact temperature and resulting mean grain sizes.[10]

Summarising the literature, there are many reports on the crystallisation and grain growth kinetics of $Li_2O–Al_2O_3–SiO_2$ in general,[19–23] but so far, there are only a few publications on the crystallisation of UV-exposed Foturan®,[24–26] and detailed investigations of the nucleation and crystallisation kinetics of Foturan® are sparse. However, microfabrication would strongly benefit from a higher flexibility in the feature size through variation of the mean grain size which is achievable by variable crystallisation and grain growth conditions, and thermal annealing of these wafers to allow for the fabrication of high-temperature MEMS, such as micro-solid oxide fuel cells.[12,14] A detailed investigation of the temperature and heating-rate dependence of the nucleation and the crystallisation of Foturan® is thus essential in order to obtain an optimal number of nuclei and a controlled crystal growth rate, and to minimise the annealing time.

It is the aim of this paper to study the nucleation and crystallisation kinetics Foturan® glass–ceramic substrates. The nucleation, crystallisation and grain growth of UV-exposed Foturan® are investigated in detail by differential scanning calorimetry (DSC), X-ray diffraction (XRD) and scanning electron microscopy (SEM) in order to optimise the Foturan®

annealing programs with respect to total processing time, maximum temperatures, heating rates and dwell times to allow for small feature sizes in microfabrication with Foturan® substrates.

2. Experimental procedures

Foturan® wafers (Mikroglas Chemtech GmbH, Germany, Ø: 4 in., $300\,\mu m$ thickness) with polished surfaces were cut into smaller pieces with a wafer saw (Disco Dad 321) or by diamond carving. Two types of samples – untreated and UV-exposed Foturan® wafer pieces – were used for the crystallisation and grain growth studies. The UV-exposed samples were radiated for 4 min with a 310 nm UV light (LOT-Oriel 500 W Hg UV-Source) operating at 450 W.

Nucleation and crystallisation of the Foturan® samples were studied by a combined differential scanning calorimeter and thermogravimetric device (DSC/TG, STA 449C Jupiter calorimeter, Netzsch, Germany). In these DSC measurements, the degree of crystallinity can be obtained from integration of the exothermic heat loss signal.[20] In order to quantify the DSC results, the instrument was calibrated with calibration standards (Netzsch 6.223.5-91.2) with known melting points and heat losses, or phase changes. The pieces of Foturan® ($\sim$4 mm × 4 mm) were put into an aluminium oxide crucible (0.085 mL, outer diameter Ø 6.8 mm, Netzsch, Germany) and measured against an empty reference crucible. All crucibles were covered with a platinum lid to increase the heat conductivity. The cooling curve was used for the correction measurement, as the fully crystalline Foturan® did not show any reversible changes. Non-isothermal DSC experiments were measured from RT to $1100\,^{\circ}C$ at different heating rates with 60 mg of Foturan®, whereas in the isothermal DSC measurements 45 mg of Foturan® were sufficient. A synthetic air atmosphere of 43.7% argon and 12.3% oxygen was set during the measurement with an air flow of 60 sccm. The DSC characteristics were evaluated using the Netzsch evaluation software (Proteus Thermal Analysis, Version 4.7.0), whereby the peak temperatures were taken for the glass transition and crystallisation, and the onset temperature was used for describing the melting of the glass.

A detailed microstructural analysis at the different states of crystallisation of Foturan® was performed. For this, the 1 cm × 1 cm Foturan® samples were annealed in an oven (Logotherm® Controller S17, Nabertherm, Switzerland) with a heating rate of $3\,^{\circ}C/min$ and a cooling rate of $15\,^{\circ}C/min$ to temperatures between $400\,^{\circ}C$ and $850\,^{\circ}C$, where the actual nucleation and crystallisation of the material takes place. The crystallisation of the Foturan® samples was investigated by XRD (diffractometer D5000, Siemens, Germany) with Cu Kα radiation ($\lambda = 0.154$ nm), a beam diameter of 6 mm, an exposure time of 20 s and a resolution of 0.02. The microstructure of UV-exposed Foturan® was analysed by SEM (Leo 1530, Zeiss, Germany). All Foturan® samples were sputtered with carbon using a sputter coater (SCD 050, BAL-TEC, Liechtenstein) in an argon atmosphere of 5×10^{-2} mbar. Copper tape was used to obtain better pictures by avoiding charging effects. An acceleration voltage of 10.00 kV and a working distance of 2 mm were used.
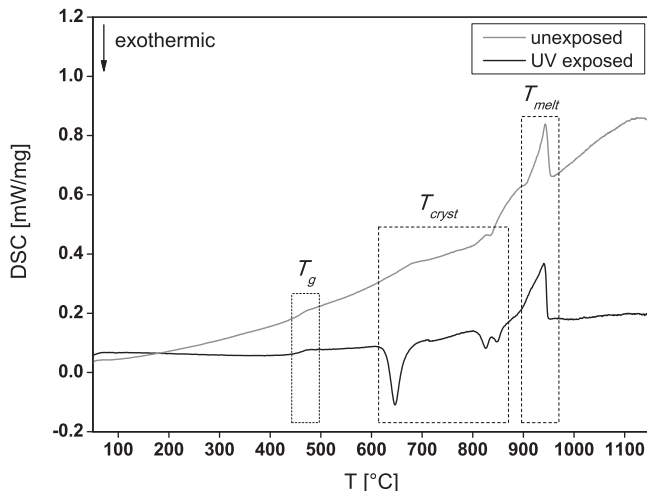
Fig. 1. Differential scanning calorimetry signals for non-isothermal crystallisation of UV-light unexposed and exposed Foturan® for a heating rate of 3 °C/min. The characteristic temperatures are denoted by the following abbreviations: T_g: glass transition temperature, T_{cryst}: crystallisation temperature, T_{melt}: melting temperature.

3. Results and discussion

3.1. Impact of the UV-exposure on the crystallisation of Foturan®

3.1.1. Non-isothermal crystallisation

The non-isothermal differential scanning calorimetry (DSC) signals for UV-light exposed and unexposed Foturan® are compared in Fig. 1 for a heating rate of 3 °C/min. Foturan® reveals equal temperatures for the endothermic signals of the glass transition temperature (T_g) at 479 °C and the melting temperature (T_{melt}) at 890 °C independent of the UV exposure. The main difference occurs in the presence of exothermic signals representing the active crystallisation for the UV-exposed Foturan® between 630 °C and 850 °C, which are absent for the unexposed material. The peak maxima for the crystallisation are at 647 °C, 826 °C and 848 °C for the UV-radiated Foturan®.

For some of the unexposed Foturan® samples, a small exothermal crystallisation peak was detected at 850 °C and is possibly caused by exposure of the glass pieces to daylight. The

baselines of these two DSC curves reveal different slopes which resulted from the usage of different sample holders and new crucibles. This change of sample holder is detected by the extremely sensitive DSC method.

For both unexposed and UV-exposed Foturan®, the glass transition peak temperature (T_g) at 479 °C and melting onset temperature (T_{melt}) at 890 °C are identical, but there are no exothermal crystallisation peaks (T_{cryst}) in the unexposed Foturan®. This is expected as without the UV-radiation step, no active Ag$^+$ ions are generated, and thus, no agglomeration to Ag nuclei takes place.[10] These results are in good agreement with the literature data: Dietrich et al.[10] measured a T_g at 465 °C and Mrotzek et al.[24] a T_g at around 470 °C for both unexposed and UV-exposed Foturan® samples at a heating rate of 10 °C/min. Regarding the crystallisation, Mrotzek et al.[24] obtained an exothermal DSC signal at 650 °C with 10 °C/min for the crystallisation of an UV-exposed Foturan® sample that was thermally pre-treated at 500 °C for 1 h. No further crystallisation peaks are visible in the reported DSC curves up to 800 °C.[24]

3.1.2. Isothermal crystallisation

Isothermal DSC experiments are performed at temperatures slightly below the start temperature of crystallisation at around 560 °C as determined from the temperature-dependent DSC curves. From such isothermal DSC studies, the time-dependent character of the nucleation and crystallisation can be gathered. The isothermal DSC curves for unexposed and UV-exposed Foturan® with respect to temperature are given in Fig. 2. No exothermal DSC signal was recorded for the unexposed Foturan® (Fig. 2(a)), whereas for the UV-exposed Foturan® an exothermal crystallisation peak evolves for isothermal hold temperatures of between 560 °C and 580 °C (Fig. 2(b)). The intensity of these crystallisation peaks increases and the crystallisation temperature range is smaller with increasing temperature: at 560 °C the crystallisation is complete after 140 min, whereas at 580 °C only 80 min are required to obtain fully crystalline Foturan®.

From these isothermal crystallisation experiments, it can be concluded that the UV-radiation at 310 nm for 4 min leads to the formation of nuclei in the Foturan® glass and to crystallisation during subsequent annealing. These results also clearly reveal that the UV-unexposed Foturan® does not form any silver
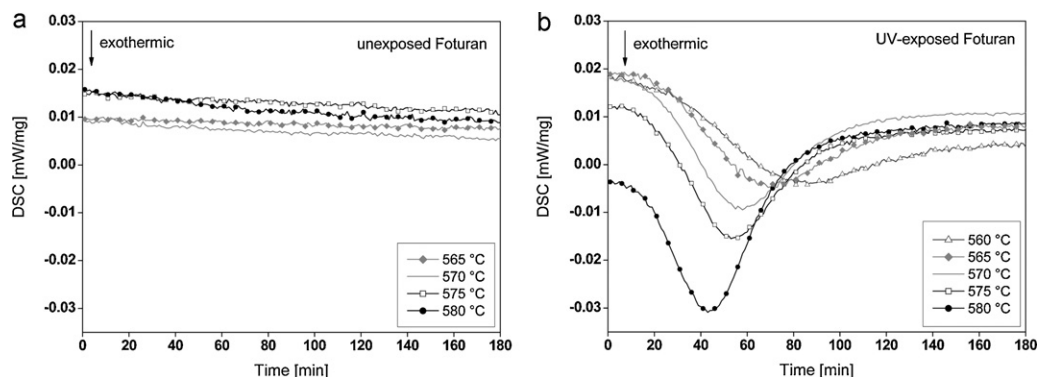

Fig. 2. Differential scanning calorimetry signals of (a) unexposed and (b) UV-exposed Foturan® for isothermal crystallisation with respect to the hold temperature. The heating rate up to the isothermal hold temperature was set to 3 °C/min.
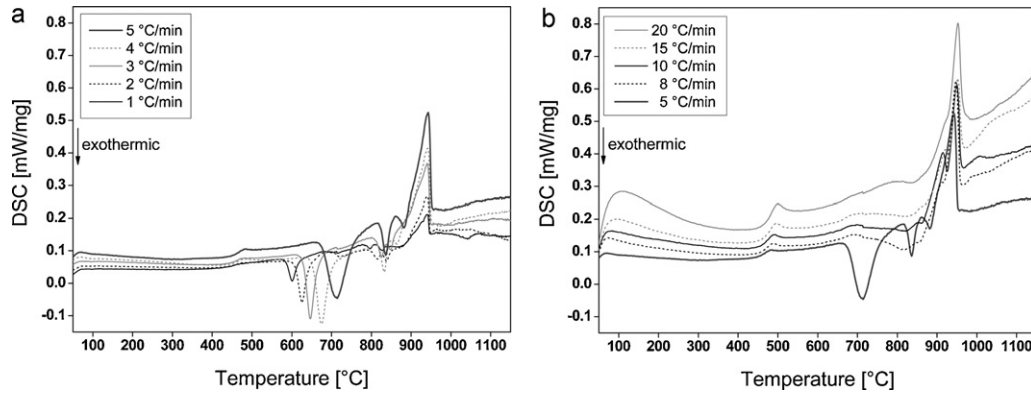
Fig. 3. Differential scanning calorimetry signals of UV-exposed Foturan® versus temperature: non-isothermal crystallisation is shown for (a) low heating rates (1–5 °C/min) and (b) high heating rates (5–20 °C/min).

nuclei and no crystallisation is induced upon thermal treatment, therefore no exothermal crystallisation peak is observed.

3.2. Crystallisation of UV-exposed Foturan®

The non-isothermal and isothermal DSC experiments in the previous sections showed that nucleation and crystallisation only take place for UV-exposed Foturan®. The photostructuring of Foturan® for MEMS applications can thus only be performed on UV-exposed samples in which amorphous and crystalline Foturan® are present. In the next sections, we will therefore only focus on the crystallisation of UV-exposed Foturan®.

3.2.1. Non-isothermal characterisation

The DSC scans of UV-exposed Foturan® samples with respect to temperature and heating rates are shown in Fig. 3. There are three main features present in the DSC curves: (i) an endothermic peak around 465 °C which corresponds to the glass transition temperature T_g, (ii) exothermic peaks which arise from crystallisation between 600 °C and 850 °C, (iii) and a further endothermic peak due to glass melting between 900 °C and 1000 °C. At low heating rates of 1–5 °C/min, Fig. 3(a), the glass transition temperature T_g, the primary and secondary crystallisation temperatures T_{cryst1} and $T_{cryst2\ a\&b}$ always increase with increasing heating rates.

Fig. 3(b) shows that for high heating rates – 8–20 °C/min – the glass transition temperature T_g increases from 489 °C to 500 °C with increasing heating rates, but no sharp exothermal

crystallisation peaks are measured around 750 °C. These heating rates are too high, so there is not enough time for nucleation and a complete crystallisation to proceed within the material.

In general, the thermal effects are much more pronounced for the high heating rates than for the low ones.[27] This is evident by the broadening, i.e. of the glass transition temperature or the crystallisation peaks, with increasing heating rates. The peak temperatures for the glass transition and crystallisation processes as a function of the heating rate are summarised in Table 1, along with the values for the enthalpy of non-isothermal crystallisation of UV-exposed Foturan®, that were determined from the area of the crystallisation peaks.

The activation energy of crystallisation of UV-exposed Foturan® was calculated with the Kissinger equation[27]:

$$\ln\left(\frac{\alpha}{T_p^2}\right) = \frac{-E_c}{(RT_p)} + Const. \tag{1}$$

where α is the heating rate [K/s], T_p is the crystallisation peak temperature [K], R is the universal gas constant [J/(K mol)] and E_c is the activation energy of crystallisation. The plot of $\ln(\alpha/T_p^2)$ vs. $1/T_p$ gives a slope $-E_c/R$ from which the energy of activation can be calculated (Fig. 4). It shows that the activation energy of the main crystallisation process T_{cryst1} (at ∼600 °C) is 1.19 ± 0.19 eV, which is 2–3 times lower than the activation energy of the secondary crystallisation processes $T_{cryst2\ a\&b}$ where $E_a = 3.76 \pm 0.08$ eV and 3.47 ± 0.18 eV. The main crystallisation process T_{cryst1} of UV-exposed Foturan® requires a

Table 1
Summary of the peak temperatures and crystallisation enthalpies for non-isothermal crystallisation of UV-exposed Foturan® with respect to heating rate (T_g: glass transition temperature, T_{cryst1}, $T_{cryst2\ a\&b}$: primary and secondary crystallisation temperatures).

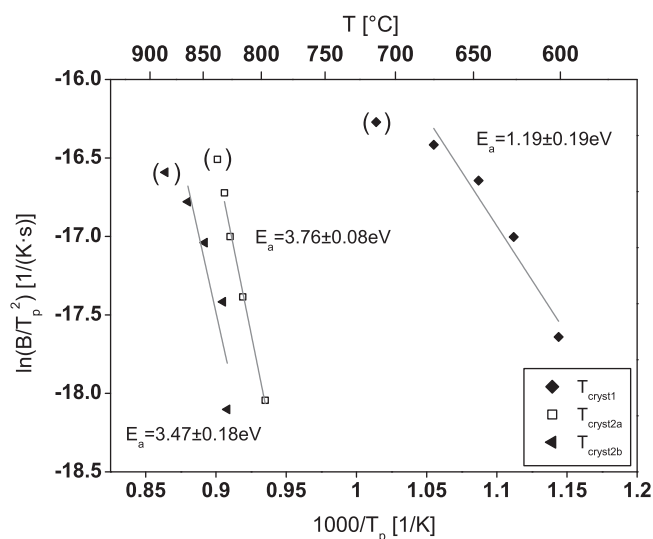| Heating rate [°C/min]	T_g [°C]	T_{cryst1} [°C]	$T_{cryst2a}$ [°C]	$T_{cryst2b}$ [°C]	ΔH_{cryst} [J/g]
1	466.1	600.9	796.3	827.6	−98.5
2	471.4	625.8	814.8	831.8	−213.6
3	478.8	646.6	826.1	847.8	−326.3
4	482.0	674.4	831.2	863.1	−413.1
5	484.5	712.6	836.6	883.6	−528.9
8	489.4				
10	492.2				
15	496.7				
20	500.3				

Fig. 4. Kissinger plot for non-isothermal crystallisation of UV-exposed Foturan®. The different crystallisation processes are given in (a). The activation energies of the different crystallisation processes (T_{cryst1}, $T_{cryst2a}$, $T_{cryst2b}$) of UV-exposed Foturan® are determined from the slopes of the linear fits. The linear fitting was done without the data from the 5 °C/min DSC curve.

lower activation energy of crystallisation than other silicate-based glasses, whereas the secondary crystallisation processes of UV-exposed Foturan® require higher activation energies of around 3.5 eV, which are similar to those of other silicate glasses.[28–30]

In Fig. 5, the crystallised fraction vs. temperature is displayed for the main crystallisation event T_{cryst1} of UV-exposed Foturan®. The crystallised fractions are resolved with respect to the heating rate by integral fractions of the exothermal peak area representing the crystallisation enthalpy (Fig. 3(a)). In the crystallised fraction versus temperature plot, a typical sigmoidal Johnson–Mehl–Avrami (JMA) curve shape similar to classical literature on glass–ceramics is obtained.[31–34] The nucleation phase – indicated by the low-temperature nonlinear correlation
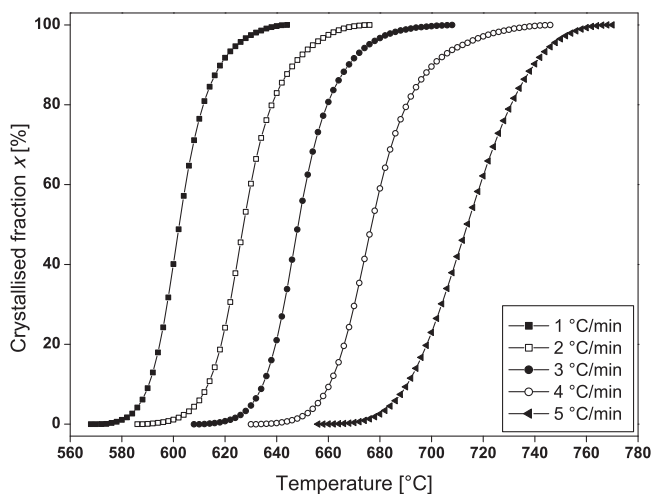

Fig. 5. Crystallised fraction versus temperature of UV-exposed Foturan® with respect to heating rate. The main crystallisation event at T_{cryst1} was taken for this analysis.
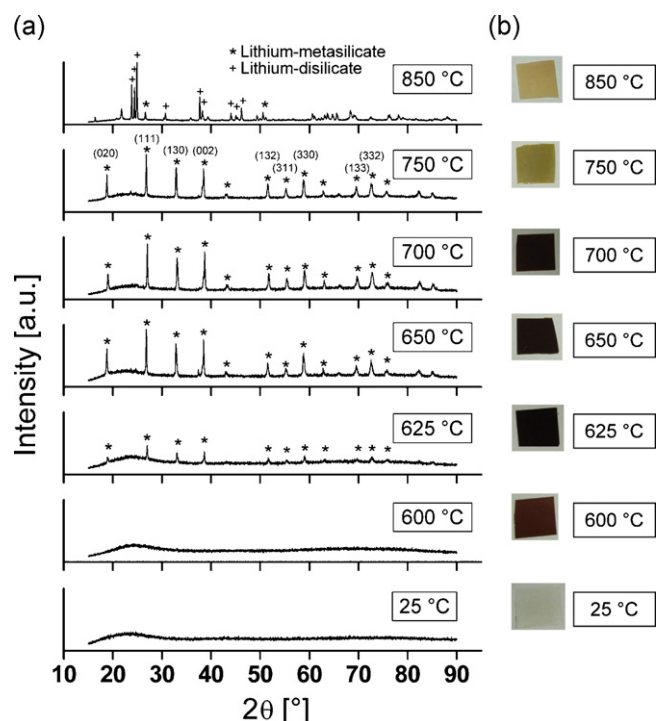

Fig. 6. (a) X-ray diffraction patterns (Cu Kα) of UV-exposed Foturan® with respect to temperature, (b) photographs showing the colour change of the UV-exposed Foturan® samples. The peaks were assigned using JCPDS card #29-828 for lithium–metasilicate and JCPDS card #40-0376 for lithium–disilicate.

between the crystallised fraction and temperature[35] at around 580 °C for 1 °C/min – proceeds within a very short temperature interval. This nucleation temperature interval increases to 660–685 °C for the highest heating rate of 5 °C/min. In contrast, the crystallisation – indicated by the linear correlation between the crystallised fraction and the temperature – proceeds over a wider temperature range of between 590 °C and 610 °C for 1 °C/min. Furthermore the slope decreases for higher heating rates. This can be correlated to the broader primary crystallisation peak in the DSC curve for 5 °C/min (Fig. 3(a)).

The non-isothermal crystallisation and grain growth of UV-exposed Foturan® was further investigated by XRD, SEM and TEM. In Fig. 6(a), the XRD patterns of UV-exposed Foturan® are displayed for the temperature range of 25–850 °C heated at 3 °C/min. Fig. 6(b) shows the colours of the Foturan® samples with respect to the annealing temperature. Below 600 °C, no diffraction peaks are present, as Foturan® is still amorphous and transparent in colour. At around 600 °C, distinctive XRD reflexes evolve due to the main crystallisation event and Foturan® turns to a brownish colour. The peaks are assigned to the lithium-metasilicate phase according to JCPDS card #29-828 and literature.[24,36,37] The main characteristic d-spacings are 4.69 Å, 3.30 Å and 2.71 Å for the (0 2 0), (1 1 1) and (1 3 0) reflexes, respectively. A thermal treatment up to 700 °C results in an increase of the XRD peak intensities, and Foturan® turns dark brown. The evolvement of secondary phases as indicated by the non-isothermal DSC experiments (Fig. 1) is noticeable at temperatures above 750 °C. The new reflexes present in the diffraction pattern at 850 °C were
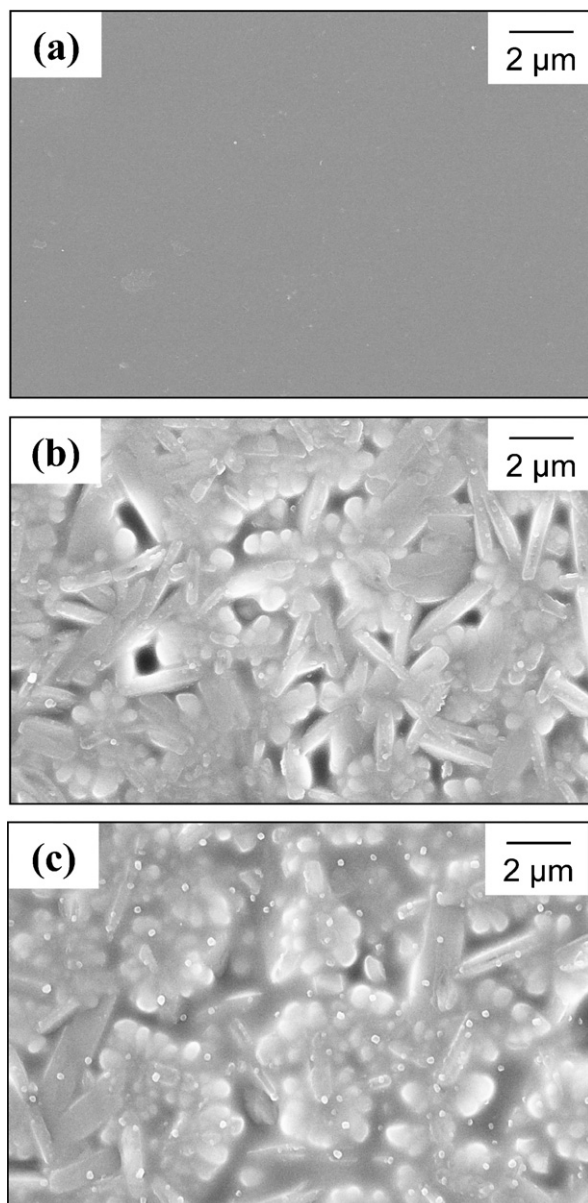
Fig. 7. Scanning electron top-view micrographs of UV-exposed Foturan® with respect to temperature: (a) 600 °C, (b) 700 °C, (c) 850 °C.

Table 2
Crystallisation enthalpy for isothermal crystallisation of UV-exposed Foturan® with respect to temperature—determined from the exothermal crystallisation peak areas of Fig. 2(b).

T [°C]	ΔH_{cryst} [J/g]
560	−53.21
565	−56.54
570	−62.77
575	−63.93
580	−71.32

assigned to the lithium-disilicate phase according to JCPDS card #40-0376.[38] Interestingly, the Foturan® colour is yellowish at this point.

The colour of the Foturan® sample reflects the state of nucleation and crystallisation of the glass: the samples annealed below 600 °C (transparent) are not yet totally crystalline; whereas the sample which was heated up to 850 °C (yellow) is completely crystalline.

It should also be mentioned that all the transparent Foturan® samples turned to a pale yellow colour after being exposed to the X-rays for several hours. The localised heat caused by the X-ray beam presumably induced a slight crystallisation of the UV-exposed Foturan® glass.

The scanning electron microscopy top-view micrographs of UV-exposed Foturan® are given in Fig. 7. At 600 °C, no crystals are visible, as Foturan® is still amorphous according to the non-isothermal DSC measurements (Fig. 1). At 700 °C, needle-shaped crystals of 1–2 μm length and 400 nm average diameter are present, and are related to the main crystallisation event. This crystal size is in agreement with the reports of Dietrich et al.[10] and Mrotzek et al.[24] who found crystal sizes of 1–10 μm. At 850 °C, the needles disappear as Foturan® starts to melt, whereby the individual grains are sintered together and that additional small grains of ∼30 nm diameter appear, which may be related to the formation of a second chemical phase during the second crystallisation process, see Fig. 3(b).

Foturan® samples with different degrees of crystallisation were also subjected to transmission electron microscopy analysis. However charging effects and changes within the photoactive glass during electron transmission made a detailed study of the microstructure impossible.

3.2.2. Isothermal characterisation

The readiness of a material to crystallise is given by its nucleation characteristics. Conventionally, these are studied via isothermal DSC measurements performed at temperatures between the glass transition T_g and the start of crystallisation T_x of the first exothermal event. The crystallisation can be induced at $T < T_x$ for longer isothermal holds, and gives an indication of its Johnson–Mehl–Avrami nucleation characteristics.[31–34] In Fig. 2(b), the isothermal DSC scans of UV-exposed Foturan® are displayed. A sharp exothermic crystallisation peak is observed for the highest isothermal temperature (580 °C). Broadening of the crystallisation peak proceeds with decreasing isothermal temperature as crystallisation takes longer to finish. Thereby the peak minimum is shifted to larger temperatures with decreasing isothermal temperature. The crystallisation enthalpies were determined from the areas of the crystallisation peaks of Fig. 2(b) and are summarised in Table 2. The crystallisation enthalpy increases with increasing dwell temperature. These results show that it is possible to crystallise Foturan® at lower temperatures than for non-isothermal crystallisation by using an isothermal hold temperature T, whereby $T_g < T < T_x$. A complete crystallisation of Foturan® can be achieved, e.g. at 570 °C after a 2 h dwell (Fig. 2(b)).

The isothermal hold temperature is thus extremely relevant for getting a large number of small grains or just a few large ones—depending on the nucleation and grain growth rates.

4. Conclusions

The nucleation and crystallisation characteristics of Foturan® glass were reported. The differential scanning calorimetry measurements showed that for unexposed Foturan® there is no exothermal crystallisation peak, whereas UV-exposed Foturan® reveals two crystallisation processes.

The crystallisation of Foturan® is heating-rate dependent and consists of one main crystallisation process between 580 °C and 750 °C with an apparent activation energy for crystallisation of 1.2 eV, determined from the Kissinger plot. At higher temperatures between 800 °C and 860 °C, additional phases appear due to secondary crystallisation processes with crystallisation activation energies of 3.4–3.8 eV. This is also in accordance with the colour changes of UV-exposed Foturan® between RT and 850 °C, indicating the different degrees of crystallisation.

It can be concluded from the non-isothermal and isothermal nucleation and crystallisation investigations that the UV-exposed Foturan® is a quite readily crystallising material. The thermal processing of Foturan® can be tailored in regards of the amount and size of nuclei and grains by the basic nucleation and grain growth characteristics reported in this study. For example, a longer isothermal hold for nucleation would lead to the formation of many nuclei, which could be followed by a fast heating rate step for short crystallisation that results in small grain and smaller feature size. This control of the crystallisation and grain growth is essential for the photostructuring and etching of Foturan® regarding the feature sizes for MEMS applications.

References

1. Stookey SD. Chemical machining of photosensitive glass. *Ind Eng Chem* 1953;**45**:115.
2. Vogel W. Chemistry of glass. Columbus, OH: The American Ceramic Society; 1985.
3. Beall GH. Design and properties of glass–ceramics. *Annu Rev Mater Sci* 1992;**22**:91.
4. Dietrich TR, Freitag A, Scholz R. Production and characteristics of microreactors made from glass. *Chem Eng Technol* 2005;**28**:477.
5. Dietrich TR, Freitag A, Scholz R. Production and properties of glass microreactors. *Chem Ing Tech* 2004;**76**:575.
6. Dietrich TR, Freitag A, Scholz R. Microreactors and microreaction systems for development and production. *mst News* 2002:3.
7. Stillman J, Judy J, Helvajian H. Aspect ratios, sizes, and etch rates in photostructurable glass–ceramic—art. no. 68820J. *Micromach Microfabric Process Technol Xiii* 2008;**6882**:J8820.
8. Stillman J, Judy J, Helvajian H. Processing parameters for the developmental of glass/ceramic MEMS—art. no. 64620A. *Micromach Technol Micro-Optics Nano-Optics V Microfabric Process Technol XII* 2007;**6462**:A4620.
9. Hulsenberg D, Bruntsch R. Glasses and glass–ceramics for application in micromechanics. *J Non-Cryst Solids* 1991;**129**:199.
10. Dietrich TR, Ehrfeld W, Lacher M, Kramer M, Speit B. Fabrication technologies for microsystems utilizing photoetchable glass. *Microelectron Eng* 1996;**30**:497.
11. Bieberle-Hutter A, Beckel D, Infortuna A, Muecke UP, Rupp JLM, Gauckler LJ, et al. A micro-solid oxide fuel cell system as battery replacement. *J Power Sources* 2008;**177**:123.
12. Muecke UP, Beckel D, Bernard A, Bieberle-Hütter A, Graf S, Infortuna A, et al. Micro solid oxide fuel cells on glass ceramic substrates. *Adv Funct Mater* 2008;**18**:1.
13. Beckel D, Muecke UP, Schoeberle B, Mueller P, Gauckler LJ. Stability of NiO membranes on photostructurable glass substrates for micro solid oxide fuel cells. *Thin Solid Films* 2009;**517**:1582.
14. Evans A, Bieberle-Hütter A, Rupp JLM, Gauckler LJ. Review on micro-fabricated micro-solid oxide fuel cell membranes. *J Power Sources* 2009;**194**:119.
15. Rupp JLM, Muecke UP, Nalam PC, Gauckler LJ. Wet-etching of precipitation-based thin film microstructures for micro-solid oxide fuel cells. *J Power Sources* 2010;**195**:2669.
16. Livingston FE, Hansen WW, Huang A, Helvajian H. Effect of laser parameters on the exposure and selective etch rate in photostructurable glass. *Photon Process Microelectron Photon* 2002;**4637**:404.
17. Anthony CJ, Docker PT, Prewett PD, Jiang K. Focused ion beam microfabrication in Foturan(TM) photosensitive glass. *J Micromech Microeng* 2007;**17**:115.
18. MacDowell JF. Nucleation in glasses. *Ind Eng Chem* 1966;**58**:38.
19. Barry TI, Clinton D, Lay LA, Mercer RA, Miller RP. The crystallisation of glasses based on eutectic compositions in the system $Li_2O–Al_2O_3–SiO_2$. *J Mater Sci* 1969;**4**:596.
20. Barry TI, Clinton D, Lay LA, Mercer RA, Miller RP. The crystallisation of glasses based on the eutectic compositions in the system $Li_2O–Al_2O_3–SiO_2$. *J Mater Sci* 1970;**5**:117.
21. Nakagawa K, Izumitani T. Metastable phase separation and crystallization of $Li_2O–Al_2O_3–SiO_3$ glasses: determination of miscibility gap from the lattice parameters of precipitated [beta]-quartz solid solution. *J Non-Cryst Solids* 1972;**7**:168.
22. Xingzhong G, Lingjie Z, Hui Y. Effects of Li replacement on the nucleation, crystallization and microstructure of $Li_2O–Al_2O_3–SiO_2$ glass. *J Non-Cryst Solids* 2008;**354**:4031.
23. Pinckney LR, Beall GH. Microstructural evolution in some silicate glass–ceramics: a review. *J Am Ceram Soc* 2008;**91**:773.
24. Mrotzek S, Harnisch A, Hulsenberg D, Brokmann U. Crystallisation mechanism in ultraviolet sensitive microstructurable glasses. *Glass Technol* 2004;**45**:97.
25. Mrotzek S, Harnisch A, Hungenbach G, Strahl H, Hulsenberg D. Processing techniques for photostructurable glasses. *Glass Sci Technol* 2003;**76**:22.
26. Hulsenberg D, Brokmann U, Hesse A, Ludwig Y, Mrotzek S. Micropatterning of glass. *Galvanotechnik* 2007:2529.
27. Kissinger HE. Reaction kinetics in differential thermal analysis. *Anal Chem* 1957;**29**:1702.
28. Xiong D, Cheng J, Li H. Composition and crystallization kinetics of $R_2O–Al_2O_3–SiO_2$ glass–ceramics. *J Alloys Compd* 2010;**498**:162.
29. Suzuki T, Arai Y, Ohishi Y. Crystallization processes of $Li_2O–Ga_2O_3–SiO_2–NiO$ system glasses. *J Non-Cryst Solids* 2007;**353**:36.
30. Shao H, Liang K, Peng F. Crystallization kinetics of $MgO–Al_2O_3–SiO_2$ glass–ceramics. *Ceram Int* 2004;**30**:927.
31. Johnson WA, Mehl RF. Reaction kinetics in processes of nucleation and growth. *Trans Am Inst Mining Metall Eng* 1939;**135**:416.
32. Avrami M. Kinetics of phase change I—general theory. *J Chem Phys* 1939;**7**:1103.
33. Avrami M. Kinetics of phase change. II. Transformation-time relations for random distribution of nuclei. *J Chem Phys* 1940:212.

34. Avrami M. Granulation, phase change, and microstructure—kinetics of phase change III. *J Chem Phys* 1941;**9**:177.

35. Jackson KA. Kinetic processes: crystal growth, diffusion and phase transformation in materials. Weinheim: Wiley-VCH; 2004.

36. Guo X-z, Yang H, Cao M, Han C, Song F-F. Crystallinity and crystallization mechanism of lithium aluminosilicate glass by X-ray diffractometry. *Trans Nonferrous Met Soc China* 2006;**16**:593.

37. Salman SM, Darwish H, Mahdy EA. The influence of Al_2O_3, MgO and ZnO on the crystallization characteristics and properties of lithium calcium silicate glasses and glass–ceramics. *Mater Chem Phys* 2008;**112**:945.

38. Soares PC, Zanotto ED, Fokin VM, Jain H. TEM and XRD study of early crystallization of lithium disilicate glasses. *J Non-Cryst Solids* 2003;**331**:217.